

Use of METEOSAT water-vapour images for the diagnosis of a vigorous stratospheric intrusion over the central Mediterranean

K Lagouvardos and V Kotroni, *University of Athens, Laboratory of Meteorology, Panepistimioupolis, Building PHYS-V, 15784 Athens, Greece*

The diagnosis of a vigorous dry intrusion over the central Mediterranean is performed using water-vapour images from METEOSAT. This dry intrusion was located on the rear side of a cold front (propagating from Italy to Greece) and played an important role in the onset of thunderstorms over the western Greek coasts. A combination of satellite imagery and potential vorticity analyses showed that the dry air originated in the lower-stratospheric and higher-tropospheric layers. The interaction of the dry air with the moist air masses within the warm conveyor belt ahead of the cold front (overrun of warm air by low equivalent potential temperature air) produced a potentially unstable region over the area of reported thunderstorms.

1. Introduction

A dry intrusion consists of a stream of dry air of upper-tropospheric and lower-stratospheric origin which, after an earlier descent, approaches the centre of a cyclone by reascending over air of high wet-bulb (or equivalent) potential temperature at low levels within the warm conveyor belt (WCB), (Young *et al.*, 1987; Browning & Roberts, 1994). Dry intrusions are a typical feature of cyclone development (Browning & Roberts, 1994) and parts of the intrusion are characterised by air with relatively high potential vorticity (PV) and low wet-bulb potential temperature, as already suggested by Danielsen (1964). High PV air within a dry intrusion is often associated with rapid cyclogenesis (Young *et al.*, 1987) when approaching a low-level baroclinic zone. In the absence of low-level forcing or baroclinic zones, but in the presence of strong upper-level forcing, a dry intrusion can still produce convective weather events.

After the onset of cyclogenesis, a dry intrusion can be identified as a cloud-free area ('dry slot') in the water-vapour (WV), infrared (IR) and sometimes in the visual (VIS) satellite images (Browning, 1997), while the dry intrusion is often evident in the WV imagery almost a day before it can be found in the IR and VIS. Thus WV imagery has been recognised as an important diagnostic tool for supplying important information in addition to that obtained from IR or VIS imagery (Mansfield, 1996). The close association of features in the WV imagery and in the PV fields has been discussed by Mansfield (1994, 1996, 1997). Although PV has been used as an operational forecast tool since the late 1980s, it is only recently that the combined use of PV and WV

imagery has been proposed for both nowcasting and for validation of Numerical Weather Prediction models (Browning, 1997; Mansfield, 1996, 1997).

Mesoscale aspects of dry intrusions associated with extra-tropical cyclones have been the subject of a series of studies (Young *et al.*, 1987; Browning & Golding, 1995; Browning, 1997; Browning *et al.*, 1997). The motivation of this study was the investigation of the applicability of existing ideas in more southerly latitudes (in the Mediterranean region) where the relationships between the water-vapour imagery and potential vorticity structures is often not well defined. Thus, in this study a dry intrusion event associated with a cold front over the central Mediterranean will be discussed based on the use of satellite imagery and upper-air analyses provided by the European Centre for Medium-Range Weather Forecasts (ECMWF).

2. Synoptic context-satellite imagery

At 0000 UTC on 20 January 1998, a low centre of 993 hPa was located in the northern Adriatic Sea. This low centre was moving south-eastwards and it was progressively filling, while it crossed the southern part of the Italian peninsula during the following hours (not shown). Figure 1 presents the mean sea-level pressure and frontal analysis at 0000 and 0600 UTC on 21 January 1998. A cold front, associated with a 996 hPa low centre, extended from southern Italy towards the northern African coasts (Figure 1(a)). Six hours later the low centre had moved south-eastwards to over the sea between Italy and Greece, while the cold front had reached the western Greek coasts. Thunderstorm activ-

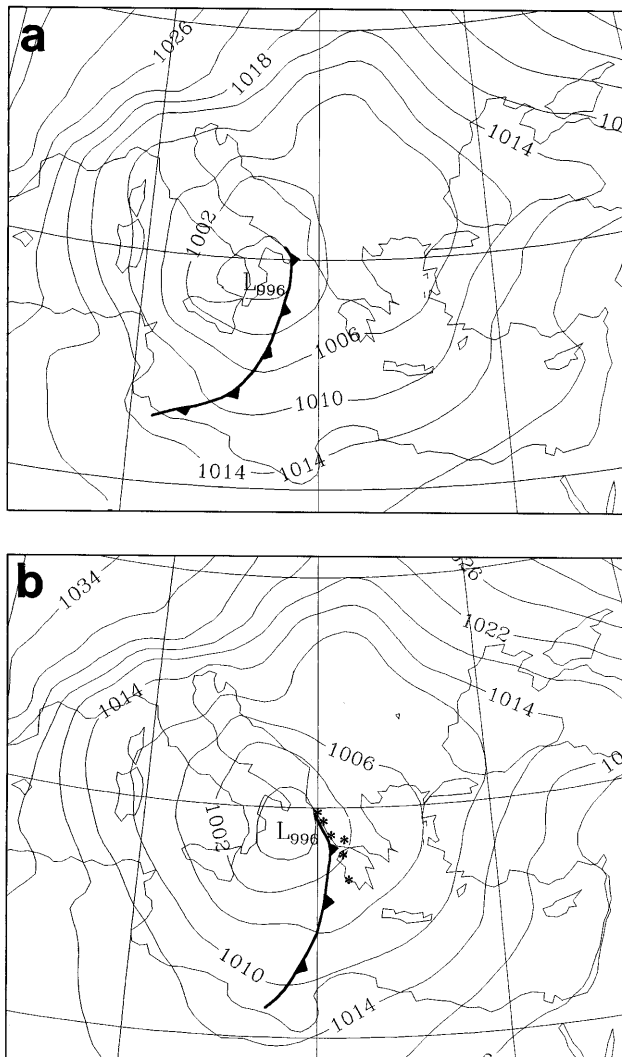


Figure 1. Surface analyses for (a) 0000 UTC and (b) 0600 UTC on 21 January 1998. Isobars are plotted at 4 hPa intervals. Cold fronts are represented with conventional symbols. Asterisks in (b) denote thunderstorm activity reported by the surface stations (at 0300 and 0600 UTC on 21 January).

ity was reported by several coastal stations in western Greece at 0300 and 0600 UTC on 21 January (denoted by asterisks in Figure 1(b)). The corresponding METEOSAT IR images are shown in Figure 2. The main features of these images are as follows.

- A broad frontal cloud band associated with the moist air within the warm conveyor belt ahead of the front. The coldest tops at 0000 UTC (Figure 2(a)) were observed over the sea, south-east of Italy, while six hours later the cloud tops penetrated deeper into the high troposphere and they were located over the western Greek coasts and central Greece (Figure 2(b)), associated with the onset of thunderstorm activity in the area.
- An almost cloud-free area situated on the western flank of the high-topped frontal cloud band. As discussed earlier, these 'dry slots' can be indicative of a dry intrusion from the upper-tropospheric

layers, but this structure is more evident in the corresponding WV images to be discussed next.

Figure 3 shows the METEOSAT WV imagery at 0000 and 0600 UTC on 21 January 1998. A well-defined broad blue zone, indicative of very low humidity within the middle and upper troposphere, is evident over the western Mediterranean. This zone narrows progressively towards the east, behind the deep band of moist cloudy air associated with the warm conveyor belt ahead of the cold front (orange and red colours). The dry slot depicted in the WV imagery closely resembles the dry intrusions over the eastern Atlantic reported in recently published research work (e.g. Browning & Golding, 1995; Mansfield, 1996; Browning, 1997). Superimposed on the WV images is the height of the 1.5 PVU surface (PVU: potential vorticity unit, equivalent to $10^{-6} \text{ m}^2 \text{ s}^{-1} \text{ K kg}^{-1}$). As discussed by Mansfield (1996), the height of the PV surface rather than its potential temperature is preferred as a diagnostic tool, because it directly indicates the degree to which the upper-level high PV is likely to influence the low-level flow. Although the 2 PVU surface has been proposed to represent the dynamical tropopause (Hoskins *et al.*, 1985), further south from the polar front region the 1.5 PVU surface seems to be more representative. At 0000 UTC on 21 January, the 1.5 PVU surface extends down to 635 hPa (Figure 3(a)), indicating that the air within the dry zone originated from the lower stratosphere/upper troposphere.

Six hours later (Figure 3(b)), the 1.5 PVU surface just behind the cold front is found at the 520 hPa level. The minimum height of the 1.5 PVU surface is positioned slightly to the west of the dry slot. Although PV anomaly is commonly found to the rear of the darkest parts of the imagery at the start of the deepening phase, it coincides better with the darkest area as the low reaches maturity (Mansfield, 1997). It seems that in this case this slight mismatch of the PV anomaly being positioned to the west of the dry slot, can be attributed to the lack of upper-air measurements over the maritime area between Italy and Greece and also along the western Greek coasts. Indeed, Mansfield (1996) demonstrated the importance of assimilating upper-air measurement into numerical analyses for the accurate position of high PV values (minima in PVU height charts) in relation to dry slots depicted in WV imagery.

The WV imagery clearly shows the existence of a dry intrusion, but it cannot provide further information on the interaction of this dry air penetration within and/or upon the warm conveyor belt. It should be noted that the horizontal extension of the dry intrusion in the western part of the frontal cloud band and the over-running of part of the warm conveyor belt (WCB) can be masked by the vertical development of the WCB clouds. As summarised by Browning (1997), the dry intrusion can interact with the high wet-bulb potential temperature air of the WCB in different ways resulting

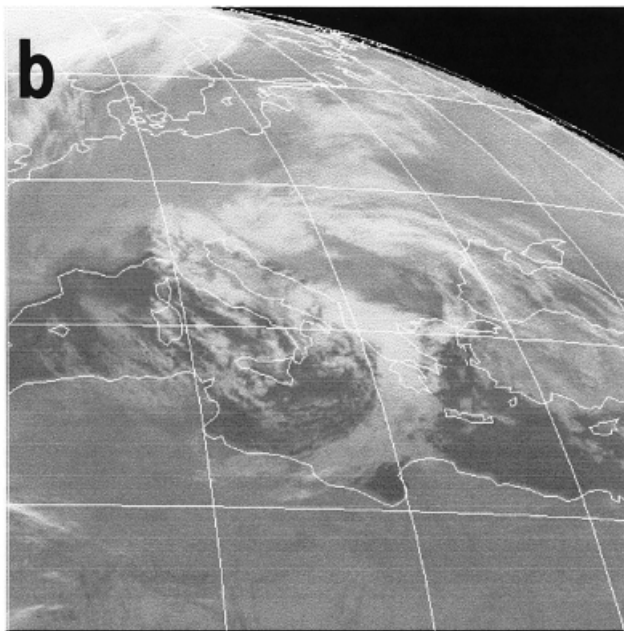
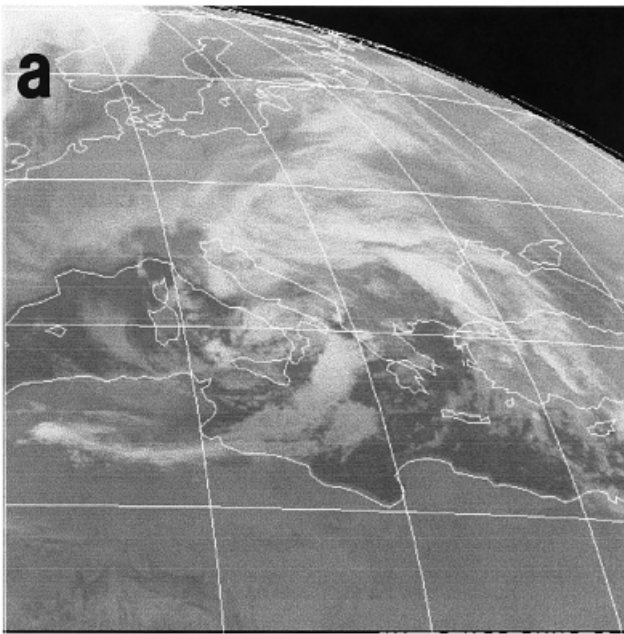


Figure 2. METEOSAT infrared images at (a) 0000 UTC and (b) 0600 UTC on 21 January 1998. These images correspond to the analyses given in Figure 1.

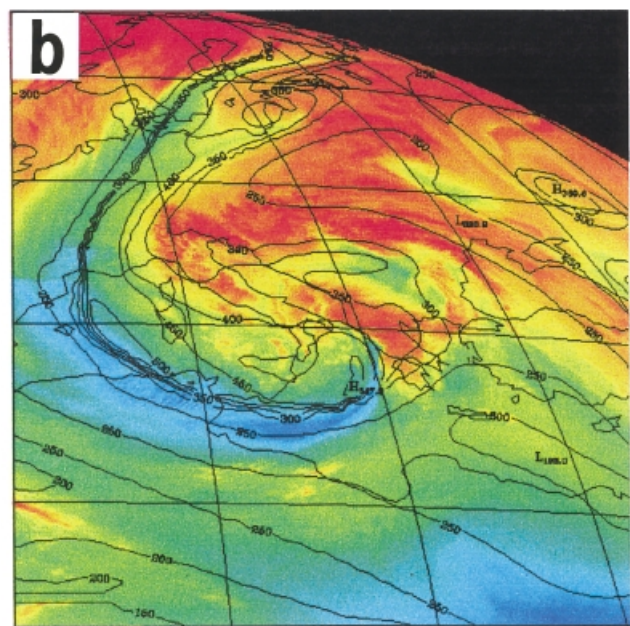
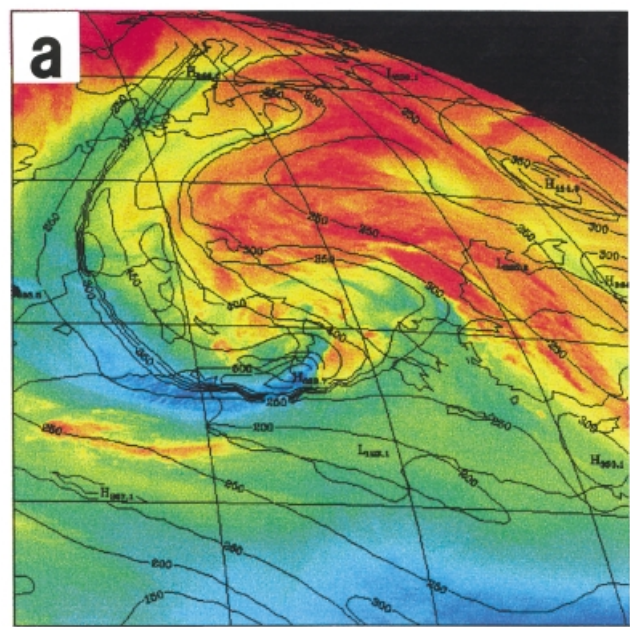


Figure 3. METEOSAT false-colour water-vapour images at (a) 0000 UTC and (b) 0600 UTC on 21 January 1998. The driest regions are coloured blue. Superimposed are the 1.5 PVU-surface pressure levels (at 50 hPa intervals), computed from the ECMWF analyses.

in different frontal archetypes. These range from the pure kata-front case, where the dry-intrusion air overruns the WCB air, leading to a split cold front (Browning & Monk, 1982), to the pure ana-front case where the dry intrusion undercuts an extrusion of the upper part of the WCB air, thus overrunning the lower part of it, producing potential instability and generating a wide rainband behind the narrow cold frontal rainband. Browning & Golding (1995), on the basis of weather radar imagery and mesoscale model results, have put into evidence this undercutting of the upper part of the WCB air by a dry intrusion (see their Figure

10(b)). For the present case, the eventual overrun of the lower part of the WCB by the dry intrusion cannot be studied owing to the lack of radar data and mesoscale model analysis; only some indications can be gained through inspection of vertical cross-sections, discussed in section 3.2. ECMWF analyses and surface observations did not show any deepening of the surface low; this leads to the conclusion that there was no large-scale interaction of upper- and lower-level forcing. Nevertheless, the dry intrusion produced a local region of potential instability, as indicated by the thunderstorm activity on the eastern edge of the dry intrusion.

3. The dry intrusion as depicted from ECMWF analyses

3.1. Horizontal cross-sections

ECMWF analyses with the maximum available horizontal resolution (0.5×0.5 lat/long) provide a very useful tool for the study of the horizontal and vertical structure of the dry intrusion. Figure 4 shows relative humidity field at the 700 hPa level, valid at 0600 UTC on 21 January 1998. The high values of the relative humidity field are in very good agreement with the IR image (Figure 2(b)), indicating values greater than 70–80% in the area of the frontal cloud band. A second interesting feature is the very good representation by the ECMWF analysis of the dry intrusion, with a pronounced dry tongue (relative humidity values less than 30%) behind the front, curving north-eastwards over the sea south-west and west of the Greek Peninsula. Inspection of a series of relative humidity fields at different pressure levels (not shown) revealed that this dry area is mainly found above the 700 hPa level, while the lowest tropospheric layers have relative humidity values greater than 70% in the area of the dry intrusion. Thus the dry air has not descended deeper than the 700 hPa level; this structural feature will also be found in the vertical cross-section of the relative humidity discussed in section 3.2.

The wind flow, relative to the moving system, at the same level, reveals a strong flow along the major WCB axis and an even stronger inflow of air within the area of the dry intrusion. Indeed, the relative flow within the dry intrusion exceeds 20 ms^{-1} . The inflow terminates over the south-eastern edge of Italy at the centre of the low. This pattern is similar to that presented by Browning & Golding (1995, Figure 3) and Browning (1997, Figure 6(a)).

3.2. Three-dimensional perspective and vertical cross-sections

A three-dimensional perspective of the dry intrusion characteristics is depicted in Figure 5. The horizontal domain of this figure is the same as that in Figure 4, but it is bounded vertically at a height of 13 km. The dry intrusion is characterised by relatively high PV air emanating from the upper-tropospheric layers and lower-stratospheric layers. Although PV values greater than 2 PVU are typical of stratospheric air near the polar front region, values of 1.5 PVU should be more typical for the central Mediterranean. Note the characteristic downward protrusion of the 0.5 PVU contour at low levels terminating inside the WCB air mass (represented by the humidity isosurface exceeding 90%, coloured in grey). These high PV air masses are characterised by low relative humidity (note that the 1 PVU contour line corresponds to a relative humidity of less than 30%). The relationship between the dry intrusion

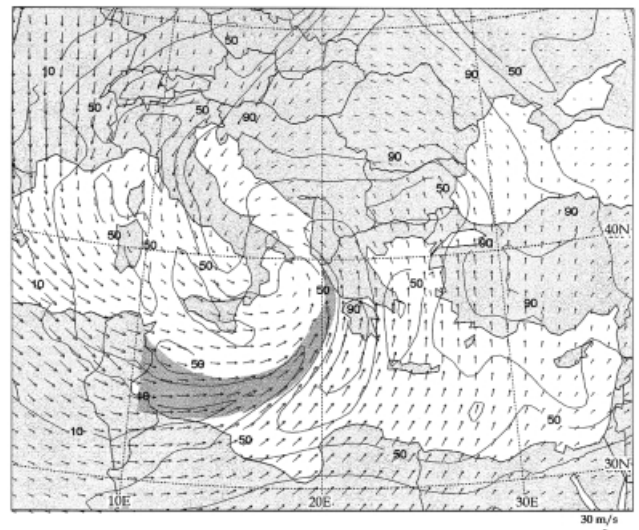


Figure 4. Horizontal cross-section of relative humidity (at 20 % contour interval), and wind flow, relative to the moving frontal system (propagating at 11 ms^{-1} from 300°), at the 700 hPa level at 0600 UTC on 21 January 1998. Shading denotes the eastern edge of the dry intrusion, as deduced from the water-vapour image depicted in Figure 3(b).

and the PV and humidity distribution in the vertical presented in this case is very similar to the one presented by Browning (1997, Figure 6(b)). With regard to the cloud development (relative humidity exceeding 90%), the clouds associated with the WCB represent the most important vertical development over the western part of continental Greece, in the area where thunderstorm activity was reported by the surface stations.

4. Concluding remarks

In this study a description has been given of the structure of a vigorous dry intrusion over the central Mediterranean. The description was based on the use of METEOSAT WV images and ECMWF upper-air analyses. The dry intrusion was detected as a dry slot in the WV imagery located on the west side of the frontal cloud band. Inspection of the ECMWF analyses revealed that the dry intrusion was characterised by a potential vorticity maximum, and near the central part of the intrusion the 1.5 PVU surface (approximately representing the dynamical tropopause) was found down to 640 hPa.

Inspection of the evolution of sea-level pressure revealed that this intrusion did not result in a deepening of the low centre, indicating that the upper-level forcing did not introduce a low-level forcing. Nevertheless, there are indications that as this low equivalent potential temperature air penetrates within the warm and moist conveyor belt, leaving part of the high equivalent potential temperature air below the dry

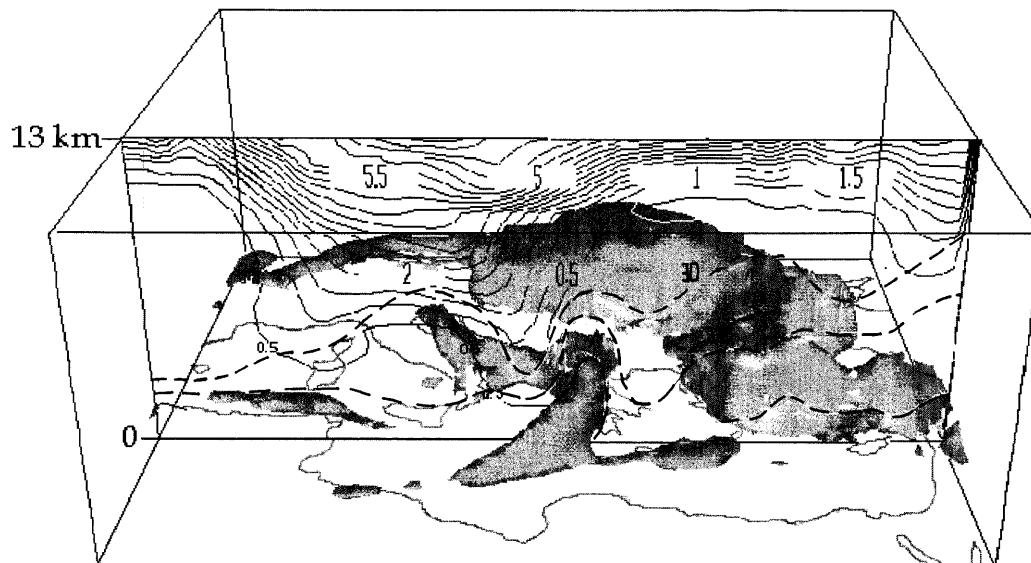


Figure 5. Three-dimensional view of the domain shown in Figure 4. Humidity exceeding 90% is coloured grey. Solid lines show potential vorticity (at 0.5 PVU intervals) and dashed lines relative humidity (at 20% intervals) on a cross-section following approximately the 35° N latitude line.

intrusion, a region of potential instability and convection is generated locally. This feature has been discussed in many recent publications. A further investigation of the dry intrusion overrunning part of the WCB would necessitate the availability of radar data and/or the use of mesoscale model results.

The three-dimensional perspective of the dry intrusion showed very well the penetration of upper-tropospheric air into the lower troposphere, descending toward the position of the surface cold front. Although the ECMWF analyses do not show the full extent of the penetration of the dry air within the WCB, the thunderstorm activity reported from at least four synoptic stations in this area indicates that such a penetration did occur. This feature cannot be seen in the WV images because cold-top WCB clouds can mask the low relative humidity air associated with the intrusion. This interaction between the dry intrusion and the WCB air is shown schematically in Figure 6. The dashed line depicts approximately the horizontal extent of the dry intrusion within the WCB air, while asterisks denote the reported thundery activity. It is evident that thunderstorms were observed at the leading edge of the dry intrusion, where potential instability was released. Roberts (1995) reported a similar case where the onset of thunderstorms coincided in space with the area where the dry intrusion interacts with the cold front cloud band.

As a final remark, this study provided further support to the well-established idea that METEOSAT WV images are very helpful in identifying the dry air emanating from the lower stratosphere and constitute a very useful tool for the determination of areas where thunderstorm activity can be expected.

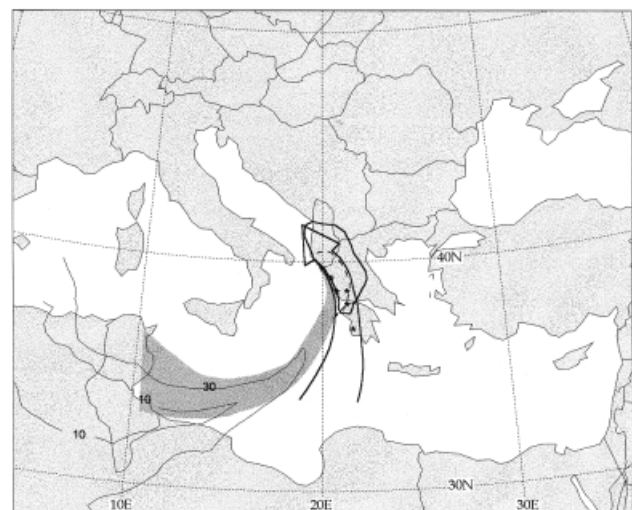


Figure 6. Conceptual scheme of the interaction of dry intrusion with the WCB air, representative of the situation at 0600 UTC on 21 January 1998 (zoom inside the domain shown in Figure 4). Dark shading denotes the eastern edge of the dry intrusion, as deduced from the water-vapour image. The 10% and 30% contour lines of relative humidity at the 700 hPa level (lower level of dry air penetration) are also shown. Convective clouds associated with the WCB are depicted by a bold line. The dashed line represents the suggested intrusion of dry air within the WCB air (represented with the open arrow) while reported thunderstorms (at 0300 and 0600 UTC on 21 January) are indicated with asterisks.

Acknowledgements

The authors are grateful to the Hellenic National Meteorological Service (HNMS) and especially to Mr G. Potiriadis for providing the METEOSAT data used in this study. HNMS is also acknowledged for the surface data used in this paper. The authors are also grate-

ful to Dr G. Kallos (University of Athens, Lab. of Meteorology) and to D. Ziakopoulos (Central Forecasting Office, HNMS) for fruitful discussions. Special thanks are also due to the editor R. W. Riddaway for his suggestions, which led to the improvement of the English and clarity of the text.

References

- Browning, K. A. (1997). The dry intrusion perspective of extra-tropical cyclone development. *Meteorol. Appl.*, **4**: 317–324.
- Browning, K. A. & Monk, G. A. (1982). A simple model for the synoptic analysis of cold fronts. *Q. J. R. Meteorol. Soc.*, **108**: 435–452.
- Browning, K. A. & Roberts, N. M. (1994). Structure of a frontal cyclone. *Q. J. R. Meteorol. Soc.*, **120**: 1535–1558.
- Browning, K. A. & Golding, B. W. (1995). Mesoscale aspects of a dry intrusion within a vigorous cyclone. *Q. J. R. Meteorol. Soc.*, **121**: 463–493.
- Browning, K. A., Roberts, N. M. & Illingworth, A. J. (1997). Mesoscale analysis of the activation of a cold front during cyclogenesis. *Q. J. R. Meteorol. Soc.*, **123**: 2349–2375.
- Danielsen, E. F. (1964). Project Springfield Report, Defence Atomic Support Agency, Washington D.C. 20301, DASA 1517 (NTIS # AD – 607980), 97 pp.
- Hoskins, B. J., McIntyre, M. E. & Robertson, A. W. (1985). On the use and significance of isentropic potential vorticity maps. *Q. J. R. Meteorol. Soc.*, **111**: 877–946.
- Mansfield, D. (1994). The use of potential vorticity in forecasting cyclones: operational aspects. In *Proc. of Conference on the Life Cycles of Extratropical Cyclones*, Vol. III, 27 June – 1 July 1994, Bergen, 326–331.
- Mansfield, D. (1996). The use of potential vorticity as an operational forecasting tool. *Meteorol. Appl.*, **4**: 305–309.
- Mansfield, D. (1997). The use of potential vorticity and water vapour imagery to validate numerical models. *Meteorol. Appl.*, **3**: 195–210.
- Roberts, N. (1995). Association of sferics with a dry intrusion in METEOSAT imagery. *Meteorol. Appl.*, **2**: 109–112.
- Young, M. V. (1997). Extratropical cyclones – a forecaster's perspective. *Meteorol. Appl.*, **4**: 293–300.
- Young, M. V., Monk, G. A. & Browning, K. A. (1987). Interpretation of satellite imagery of a rapidly deepening cyclone. *Q. J. R. Meteorol. Soc.*, **113**: 1089–1115.